Eur. Phys. J. AP **15**, 123–133 (2001)

THE EUROPEAN PHYSICAL JOURNAL APPLIED PHYSICS

Model of the homogeneous electrical discharge

S. Vongphouthone, H. Piquet[a], and H. Foch

Laboratoire d'Électrotechnique et d'Électronique Industrielle, Unité Mixte de Recherche INPT-ENSEIHT/CNRS, BP 7122, 2 rue Camichel, 31071 Toulouse Cedex 7, France

Received: 20 December 2000 / Revised and Accepted: 18 May 2001

Abstract. This paper is aimed at the modelling of an electrical discharge controlled by mean of a dielectric barrier, at atmospheric pressure; we focus our study on the homogeneous "regime". This model is based on the use of equivalent electrical circuits and is taking into account the main phenomena of the discharge. We also offer a method for the determination of the parameters of the model; the comparison of the experimental waveforms with the simulated ones is validating the accuracy of the proposed model in the case of discharges in nitrogen or helium. Our model is exploited to point out the drastic importance of the electrical characteristics of the power supply with respect to the main waveforms of the discharge.

PACS. 52.80.Hc Glow; corona – 84.30.Jc Power electronics; power supply circuits – 84.30.Bv Circuit theory (including computer-aided circuit design and analysis)

1 Introduction

Recently, techniques involving discharges controlled by dielectric barrier have been developed. Homogeneous discharges at atmospheric pressure, so called glow discharges, are obtained in helium, nitrogen or argon [2–5]. They are interesting in various industrial applications such as surface treatment or film deposit [3,5]. However, an electrical discharge in an ionised environment, associated with its electrical supply, constitutes an extremely complex system. Modelling is a powerful tool for describing the discharge evolution and for better understanding and predicting the involved processes. We propose to model the electrical discharge by mean of equivalent electrical circuits. The discharge mechanisms as well as the main parameters that define the operating conditions are taken into account. Depending upon the chosen conditions, it permits to predict the associated waveforms. This approach also enables to take into account the main characteristics of the electrical generator and to point out the major influence of this apparatus on the operating conditions of the discharge. On the basis of this analysis, one will be able to distinguish the important parameters of the system and of the supply, hence to choose them according to the expected performances.

[a] e-mail: piquet@leei.enseeiht.fr

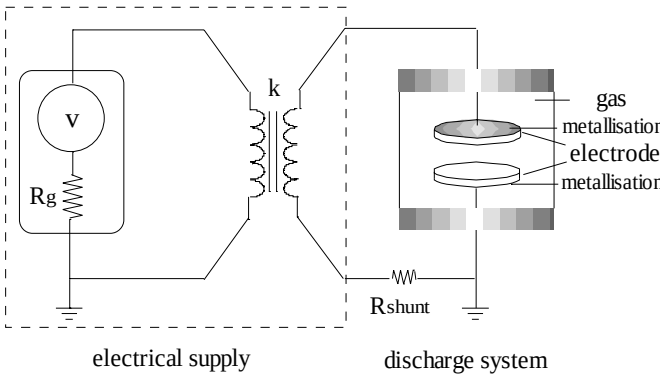

Fig. 1. Experimental device.

2 Experimental device - regimes of the discharge

Our approach is based on the analysis of the experimental waveforms, which are obtained by mean of an experimental device, which is described in this section.

2.1 Experimental device

The experimental device, which was used in our study, is presented in Figure 1 [3].

The power supply is made of a low frequency generator whose magnitude and frequency are adjustable, associated with a linear amplifier; this one has a few ohm internal resistance R_g. A lifting transformer is added in order to

provide the high voltage required by the load. Its transformation ratio is 80 for the tests in helium and 150 in nitrogen. The discharge system is composed of a reactor, which contains a gas at controlled atmosphere (helium or nitrogen) at atmospheric pressure [3]. Two circular and identical alumina electrodes are facing each other in the reactor and are separated by an adjustable gap. Both are connected to the power supply. The diameter of the electrodes used in helium is worth 4 cm and that of the electrodes used in nitrogen 12 cm. In both cases their thickness is 0.64 mm. The face connected to the supply's circuit is metallized whereas the other face is in touch with the gas. A low value resistance R_{shunt} is inserted in the circuit in order to measure the discharge current.

2.2 Discharge regimes

According to selected operating conditions, the electrical discharges obtained can evolve into two distinct regimes [2–5]:

Filamentary discharge. This kind of discharge is composed of a multitude of discharge channels (streamers). Each streamer has a relatively short lifetime of approximately 10 ns; its radius is 0.1 mm. During the first half of each half-cycle of the applied voltage the current shows many peaks of a few milliampere magnitude, with duration comparable to the streamers' lifetime. Figure 2 presents the waveforms of the discharge current; both helium and nitrogen are considered.

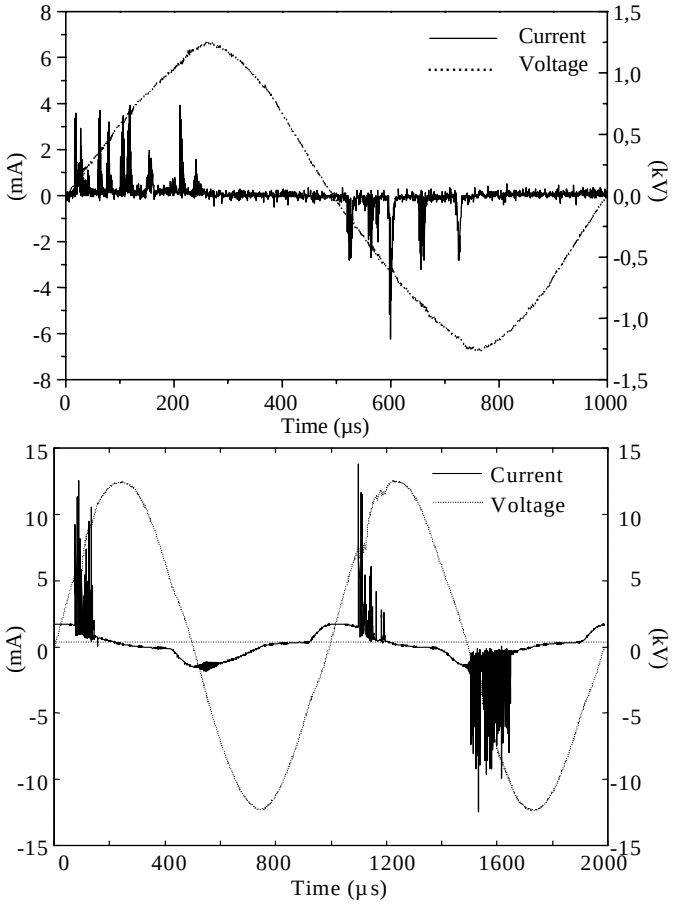

Fig. 2. Filamentary discharge: experimental waveforms of current and applied voltage at 1 kHz in helium and nitrogen.

Glow discharge regime. Glow discharge features are rather different from the filamentary discharge. These discharges uniformly cover the whole surface of the electrode. A luminous area located close to the cathode appears and moves from one electrode to another. When the sign of the applied voltage changes, the electrode polarity is indeed inverted. The cathode becomes the anode and *vice versa*. Figures 3a and 3b present experimental waveforms for helium and nitrogen. During the first part of each half-cycle, one can observe a single current peak of variable duration. In the case of helium, each peak is followed by a quite visible current-tail.

In the following, we only consider the glow discharge case.

3 System modelling

The discharge system modelling is able to highlight the role of each element of the device in discharge evolution. The discharge is modelled with an equivalent electrical circuit in order to simulate the whole system (the supply associated with the discharge) in a unique simulation environment.

3.1 Electrical discharge modelling

As we only consider the glow discharge regime, the operating conditions of each point in the inter-electrode space are assumed to be identical and synchronous; the discharge can be represented with a lumped parameters model. In order to build our model we consider that the gas obeys the following elementary rules:

- The speed of the ionised particles in the gas is proportional to the gas-voltage V_{gas}.
- In quasi-stationary conditions, the current in the discharge $I_{\text{discharge}}$ is proportional to the ionisation density; in transient conditions, these two quantities verify the following equation:

$$\tau \times \frac{\mathrm{d}\rho}{\mathrm{d}t} + \rho = kI. \tag{1}$$

  One can notice that this formulation implies that, when the discharge turns off, the ionisation density does not immediately disappear; a given quantity remains, which is gradually eliminated by recombination.
- The current in the discharge I, the voltage across the gas V_{gas} and the ionisation density are bonded in the

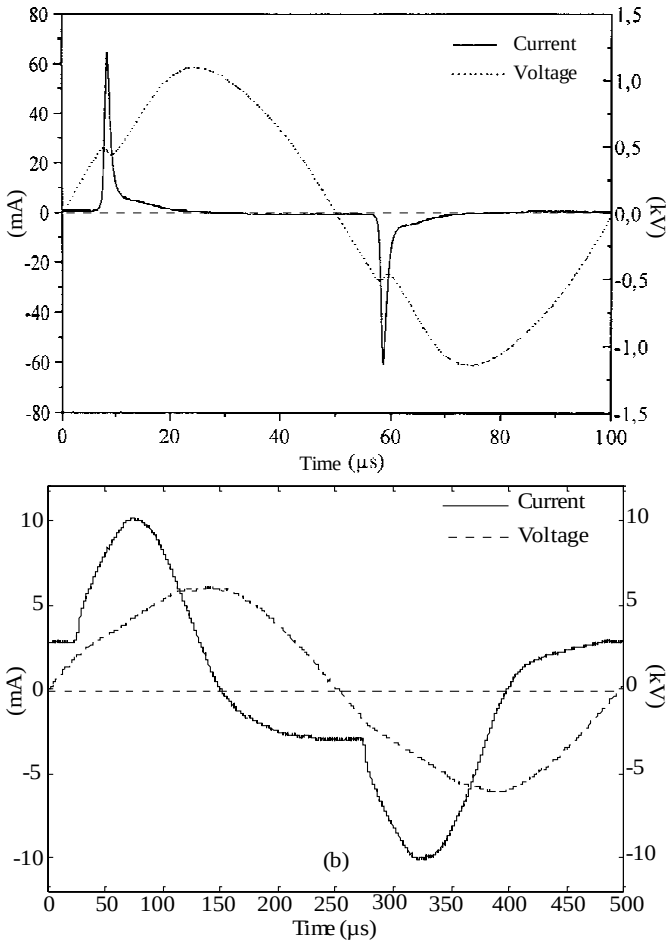

Fig. 3. Glow discharge: experimental waveforms of the current and applied voltage in helium (a) at 1 kHz and nitrogen (b) at 2 kHz.

following formula, where G is a constant:

$$V_{\text{gas}} = G \times \frac{I}{\rho} \cdot \tag{2}$$

– The breakdown voltage V_{br} of the gas is a decreasing function of the ionisation density; in a first approximation, we consider a linear relation:

$$\Delta V_{\text{br}} = K_{\text{v}} \times \rho. \tag{3}$$

These relations remain true when the discharge is in on state as well as when it is in off state.

3.1.1 Static modelling of the gas

We are using the well-known static characteristic, non-linear in the voltage-current coordinates (Fig. 4).

Without considering the arc-domain, this characteristic can be represented in electric terms as follows:

– A high value R_{off} resistor when the discharge is in off state;

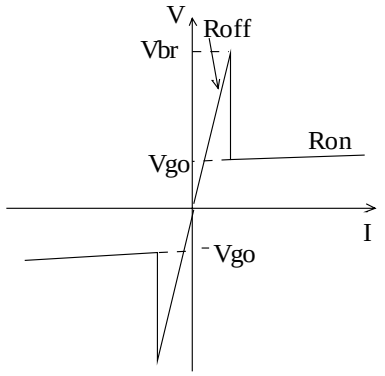

Fig. 4. Non-linear static characteristic of the discharge.

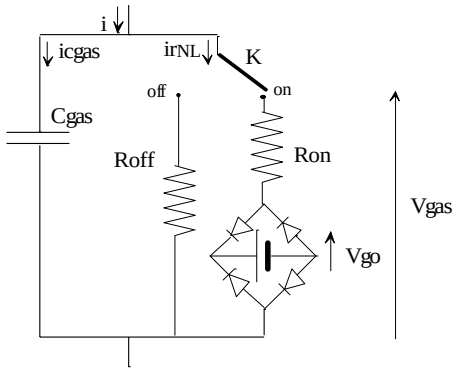

Fig. 5. Electrical equivalent circuit of the discharge.

– a small value R_{on} resistor associated with a voltage source V_{g0} when the discharge is in on state.

The operation of the discharge can be described, in sequential terms, as follows: starting from null initial conditions, it turns on when the voltage across the gas reaches the breakdown voltage V_{br}. The operating point jumps from the R_{off} branch of the characteristic to the R_{on} one. The discharge turns off when the current crosses the null value. Figure 5 presents the equivalent circuit of the discharge; the switch K toggles to the "on" or "off" state according to the described conditions.

One can notice in this circuit a capacitor, C_{gas}, which has not yet been mentioned; it is connected in parallel with the previously described circuit: when the discharge is in off-state, the gas behaves like an insulator, and the system can be modelled as a capacitor. The current in this component is provided by the power supply, but is not considered as a part of the current in the discharge.

3.1.2 Dynamic model of the gas

As soon as the voltage across the gas reaches the V_{br} value, a breakdown occurs in the gas. The initiated discharge drives a current which induces the gas ionisation (Eq. (1)) [3,5], that leads to a breakdown voltage collapse throughout the discharge duration (Eq. (3)). Once the discharge turns off and the current is cancelled, ionisation gradually disappears by recombination of charged

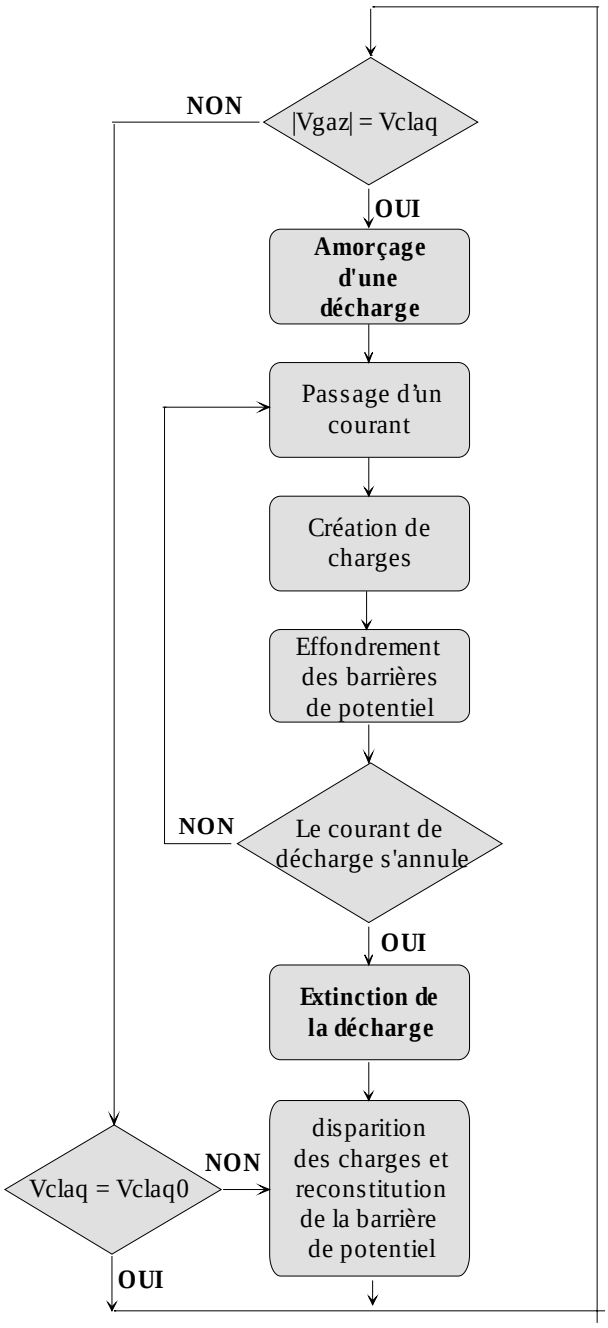

Fig. 6. Functional diagram for the management of the breakdown voltage V_{br}.

particles, which were created during the discharge lifetime. Then the breakdown voltage raises to its initial value V_{br0} if no breakdown appears before. The functional diagram of Figure 6 details the involvement of this phenomenon in the discharge evolution. The electrical circuit given in Figure 7 models this behaviour.

A $R{-}C$ circuit is excited by the absolute value of the discharge current. The output voltage across this subcircuit is the image of the resulting ionisation, as defined in equation (1). This part of the model involves a delay between the current I and the ionisation; in steady state

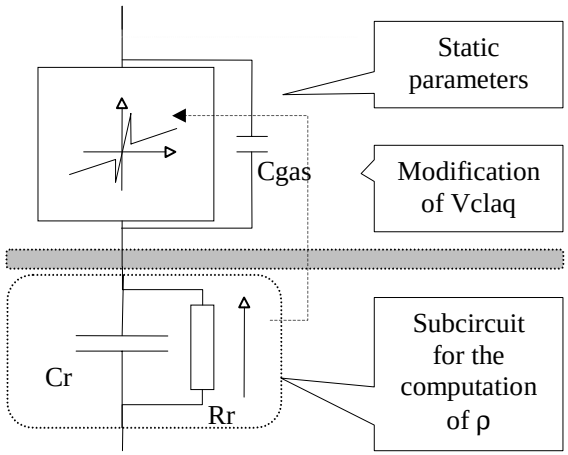

Fig. 7. Equivalent circuit for the management of the breakdown voltage.

operation, it respects the relation (Eq. (2)), as the voltage across the discharge in on state is quasi constant. This quantity is amplified by a gain K_{v} and the result represents the breakdown voltage drop due to ionisation. This one is then subtracted from the initial breakdown voltage value V_{br0}. The new breakdown voltage V_{br} is then provided to the basic discharge cell. In our voltage management model, the time-constant ($\tau = Rr \times Cr$) is adjusted to fit the ionisation's recombination phenomenon dynamics.

A simulation with this discharge model gives the ionisation evolution and the breakdown voltage associated with the discharge current (Fig. 8). We can note that the ionisation rate increases after the current flow and gives rise to the breakdown voltage collapse. This one is reconstituted gradually after the discharge's extinction. Before the next discharge's initiation, we can remark the presence of a weak ionisation, which was created during a previous discharge and had no time to disappear entirely. These charges lead to a breakdown under a new V_{br} voltage, which is weaker than V_{br0}.

3.2 Modelling of the environment of the discharge

We've just proposed a model, focused on the gas, for the behaviour of the discharge. The near environment of the later is composed of the ceramics electrodes. Only one face of these electrodes is metallized and connected to the power supply. The discharges are carried out on the other face. Between the two electrical connecting points, we represent the electrodes as a capacitor, which value is computed according to of their geometric properties and with the value of the permittivity of the ceramic. Firstly, the power supply is represented as a voltage source associated with a resistor; taking into account the transformer (which is characterised by its turns ratio K), the voltage across the source is K time the value of the voltage delivered by the linear amplifier; the resistor's value is: $K^2 R_{\mathrm{g}}$ (R_{g} being the internal impedance of the amplifier). The leakage inductance of the transformer is neglected, the voltage drop

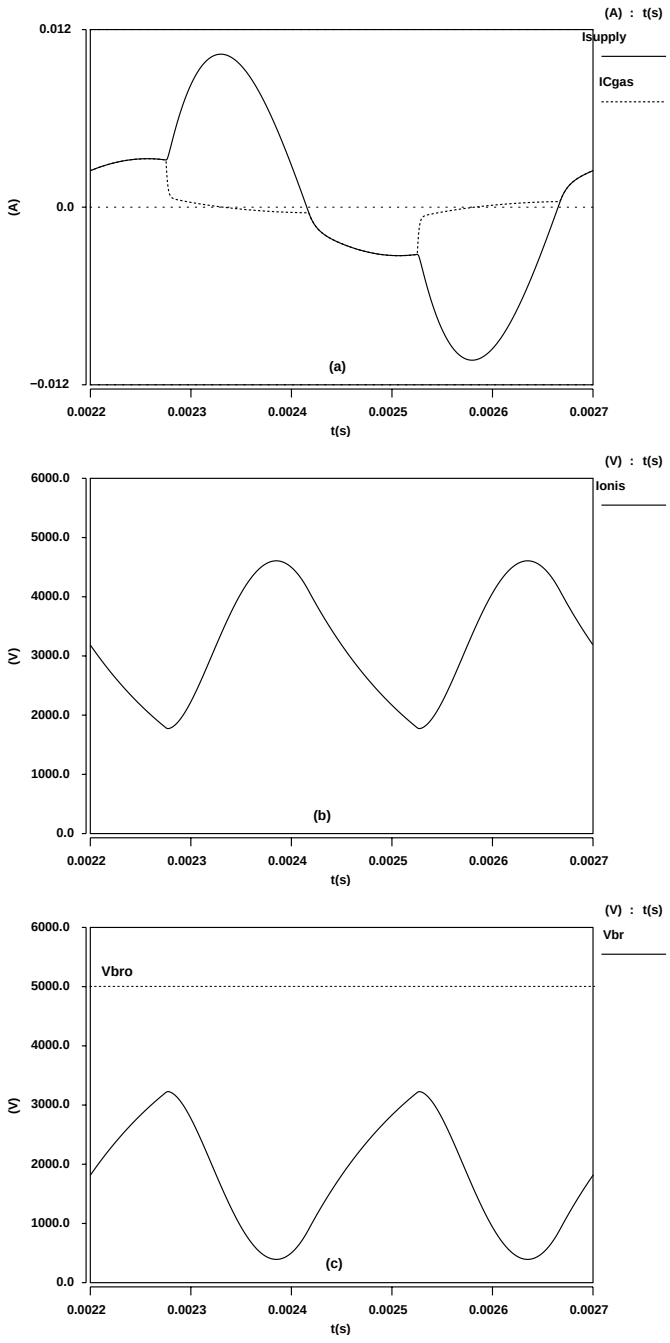

Fig. 8. Simulated waveforms in nitrogen: total current and capacitive part (a) - ionisation's image (b) - breakdown voltage (c), with initial value: $V_{\mathrm{br0}} = 5000$ V.

it causes in association with the current slope in the supply being by magnitude orders smaller than the one due to the internal resistance of the supply; nevertheless one could introduce it in the equivalent circuit to evaluate its importance. Our approach of the modelling of the whole system, by mean of equivalent circuits, is giving wide opportunities to investigate various solutions for the power supply: one can test different kinds of waveforms (by mean of ideal sources) or evaluate the performances and constraints of precisely described electronic circuits [6].

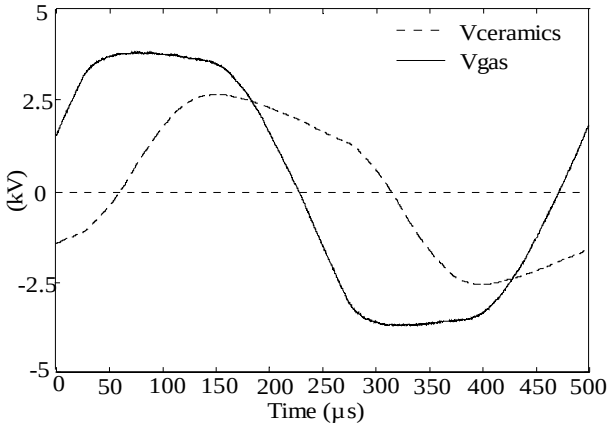

Fig. 9. Computed ceramics and gas voltages.

4 Identification of the parameters of the model

The model, which has just been described, depends upon a set of parameters. We are now presenting a method to achieve the identification of these data. We start from the experimental waveforms of the measured voltage across the terminals of the transformer and current delivered to the discharge apparatus. Let us once again remember that we consider homogeneous regime for the discharge, as the whole gas is operating in the same condition. We treat in this section the case of nitrogen (experimental waveforms of Fig. 3b) to define the parameters of the circuit presented in Figure 5.

4.1 Determination of the ceramics and gas voltages

Starting from the discharge current and the value of the ceramics capacity, we deduce the ceramic voltage. This one checks two conditions: it is proportional to the discharge current integral and its average value is null (Eq. (4)). The mesh law gives then the gas voltage (Eq. (5)). These two voltages, calculated from the experimental curves, are given in Figure 9.

$$V_{\mathrm{ceramics}} = \frac{1}{C_{\mathrm{ceramics}}} \times \int i_{\mathrm{discharge}} \mathrm{d}t + K$$
$$\langle V_{\mathrm{ceramics}} \rangle = 0 \qquad (4)$$

$$V_{\mathrm{gas}} = V_{\mathrm{supply}} - V_{\mathrm{ceramics}}. \qquad (5)$$

4.2 Parameters of the static characteristic

From the experimental waveform of the current I in the discharge and the computed voltage across the gas, we can plot the current-voltage characteristic presented in Figure 10.

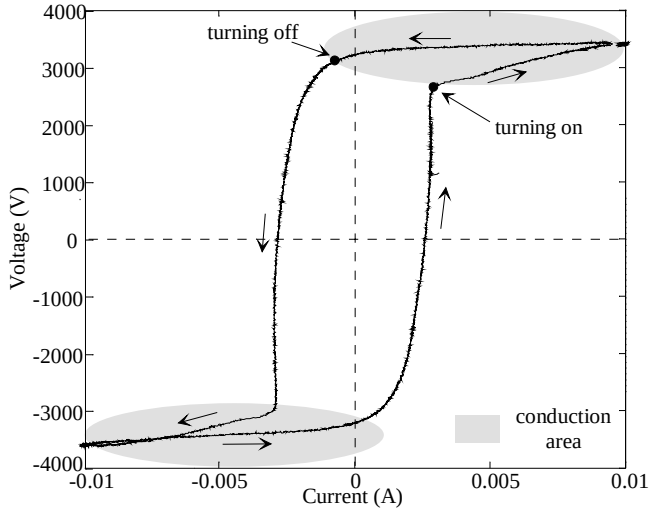

Fig. 10. Experimental characteristic: gas voltage *vs.* discharge current.

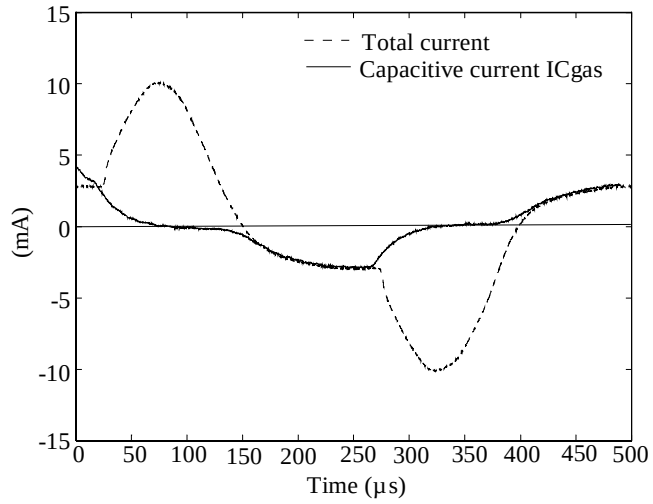

Fig. 11. Experimental total current and computed capacitive current in the discharge.

This is a dynamic characteristic whereas that of our model is static (Fig. 4). During the extinction phase of the discharge, the later has a certain thickness corresponding to the presence of a current in the gas capacity. This capacitive current checks two conditions (Eq. (6)). It is proportional to the derivative of the discharge's voltage and during the discharge extinction phase, it is equal to the discharge current.

$$I_{C_{\text{gas}}} = C_{\text{gas}} \times \frac{\mathrm{d}V_{\text{gas}}}{\mathrm{d}t}$$
$$I_{C_{\text{gas}}} = I_{\text{discharge}} \text{ (when discharge is OFF).} \quad (6)$$

By fitting the value of C_{gas}, the capacitive current of gas is superimposed on the discharge current when the discharge is turned off (Fig. 11).

In our case, $C_{\text{gaz}} = 45$ pF; this value is quite higher than the theoretical value (30 pF) which is calculated from the electrode dimensions. The difference is imputed to the parasitic capacities, which have to be added to the gas capacity (parasitic capacities between the higher electrode and the wall reactor, which is grounded, output capacitor of the supply). The gas current, which is noted ir_{NL} (non-linear resistance current of Fig. 5), resulting from the difference between the total current and the capacitive current, is computed. Then, we can draw the static voltage-current characteristic of the gas (Fig. 12).

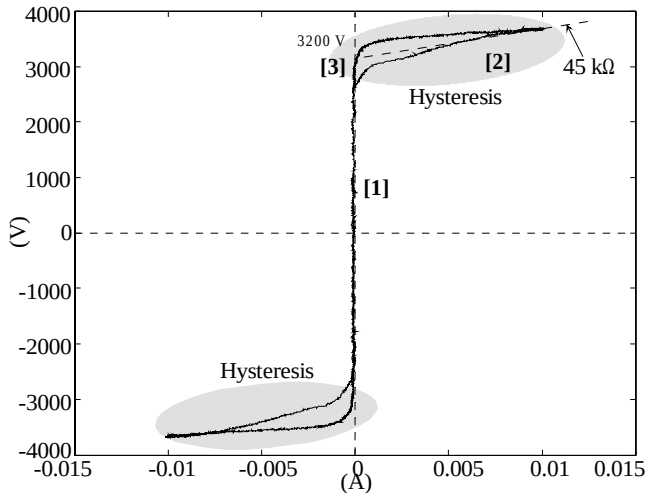

Fig. 12. Static current-voltage characteristic of the gas.

This characteristic presents a more similar shape to the static discharge characteristic. However a hysteresis phenomenon always remains during the current rise and fall. We suppose that it is caused by a charge storage phenomenon. However, we do not take it into account and use the average characteristic in order to obtain the discharge model parameters. The R_{off} resistance (off state of the discharge), corresponds to the slope of the part [1] of Figure 12; the R_{on} resistance corresponds to the part [2]. The breakdown voltage has practically the same value that the discharge's back electromotive force V_{g0} (measured at point [3]). That means that the discharge potential barriers are entirely lowered.

4.3 Dynamic properties of the gas

We just determined the parameters of the static characteristic of the gas. But the later is modified by the presence of ionisation, which may lower the breakdown voltage, depending upon the operating point. The nominal value of the breakdown voltage, V_{br0}, is a parameter, which depends upon the nature of gas and the distance between the electrodes; it can be experimentally measured: one increases the supply voltage until a breakdown occurs. Once this data is known, one measures several waveforms of V_{gas}, (Fig. 9), at a given frequency and for several values of the discharge current, obtained by modifying the input voltage. We examine the evolution of the actual breakdown voltage and deduct the reduction's ratio of the breakdown voltage as a function of the discharge current (parameter K_{v}). From the values of V_{br0} and K_{v}, the τ

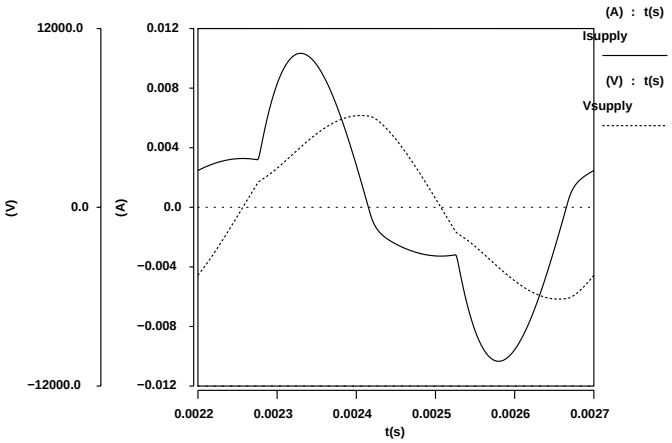

Fig. 13. Simulated waveforms of discharge's total current and applied voltage in nitrogen (2 kHz).

Table 1. Parameters of the model in nitrogen.

$R_{\rm on}$	45000 Ω
$R_{\rm off}$	20 MΩ
$V_{\rm br0}$	5000 V
$V_{\rm g0}$	3200 V
$C_{\rm gas}$	45 pF
$C_{\rm ceramic}$	220 pF
$K_{\rm v}$	3.25×10^6
τ	130 μs

Table 2. Supply's parameters.

Peak voltage (sinus)	7000 V
frequency	2 kHz
internal resistance	8 Ω
transformer's ratio	150

parameter is determined by mean of several measures, at different frequencies, corresponding to the same value of the discharge's current. These different frequencies imply different values of the duration of the off state; during the off state, the ionisation disappears by recombination, with a time-constant τ. The breakdown voltage tends to recover its nominal value, $V_{\rm br0}$, with the same time-constant τ. Measurements of $V_{\rm br}$, plotted as a function of the duration of the off state allows us to compute τ.

4.4 Parameters of the model in nitrogen

The proposed method for the identification of the parameters has been applied in the case of nitrogen (Tab. 1). The capacity of the ceramics is computed from the geometrical properties of the electrodes.

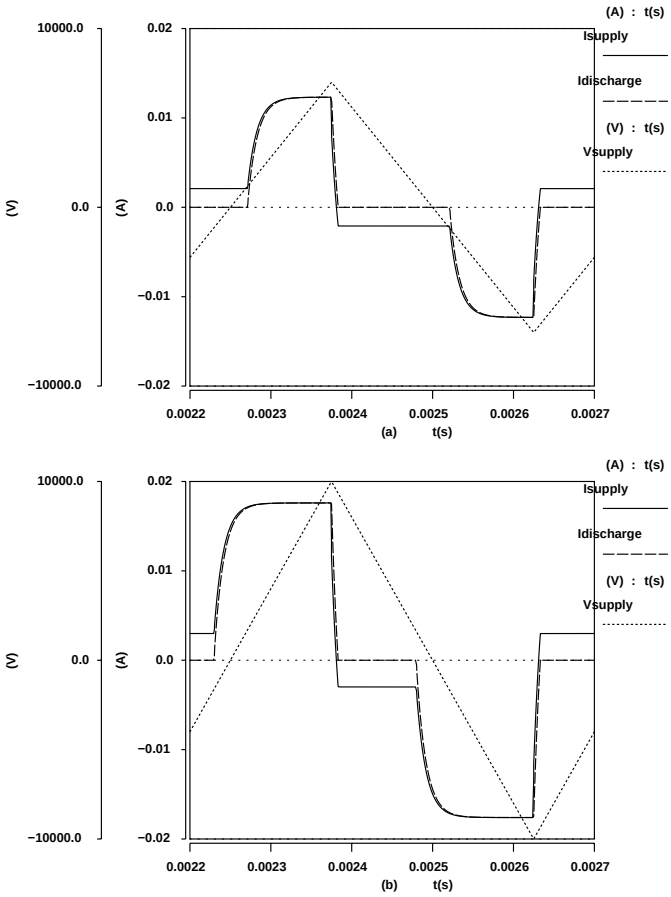

Fig. 14. Triangular voltage supply in nitrogen at 2 kHz, with 7 kV and 10 kV peak values (simulations); $R_{\rm gen} = 0$: supply's voltage and current (I, V) and current in the discharge.

5 Validation and exploitation of the models

5.1 Validation of the homogeneous discharge's model in nitrogen

With the parameters of Table 1, and the following supply parameters (Tab. 2), we simulate the experimental system with the SABER [1] simulator.

One can notice in Figure 13 the very good agreement of these results with the experimental measurements (Fig. 3b).

5.2 Supply's properties investigations

The model, which has been developed in the previous sections, makes extensive use of equivalent circuits; thus being simulated with a software devoted to the study of electrical circuits, it allows us to analyse easily the performances obtained with different kinds of supply.

5.2.1 Triangle voltage supply

In Figure 14, we present the waveforms corresponding to a triangle voltage supply; here, the resistance of the supply is not taken into account. As soon as the discharge

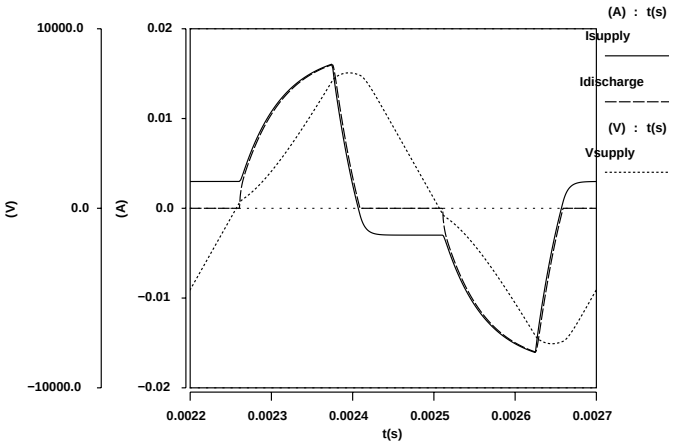

Fig. 15. Triangular voltage supply in nitrogen at 2 kHz, with 10 kV peak values and $K^2 \times R_{\text{gen}} = 180$ kΩ ((simulations): supply's voltage and current (I, V) and current in the discharge.

turns on, as the gas voltage ripple can be neglected, the dielectric barrier limits the current of the discharge and imposes the following value:

$$I_{\text{gas}} = C_{\text{ceram}} \times \frac{\mathrm{d}(V_{\text{gen}} - V_{\text{gas}})}{\mathrm{d}t} \simeq C_{\text{ceram}} \times \frac{\mathrm{d}V_{\text{gen}}}{\mathrm{d}t}.$$

As the supply's voltage, V_{gen}, is a triangle, the gas current, when the discharge is in on state, has a rectangular shape.

As it can be observed by comparison of the obtained waveforms of Figure 14, the magnitude of the rectangular part of the gas current is proportional to the slope of the supply's voltage. The discharge naturally turns off when the gas current, I_{gas}, cancels; this event corresponds to the extremum of the supply's voltage, V_{gen}.

These simulations point out that the choice of the supply is of crucial importance; the shape of the supply's voltage permits the control of the waveform of the current in the discharge, and thus the energy it receives. In order to evaluate the importance of the parasitic parameters of the supply, we have introduced in the simulated circuit the internal impedance of the generator; the simulation's results are presented in Figure 15.

One can observe that the voltage, which can be measured across the terminals of the supply, presents a voltage drop when the discharge turns on; its value corresponds to the product of the discharge current peak, by the value of the internal resistance of the generator. The value of the internal resistance of the supply (8 Ω in the previous example) corresponds to the actual equipment used in the experimental device (a linear amplifier associated with low frequency generator); this parameter is showing a negative influence on the control of the discharge current. As especially designed power supplies are able to present very low values of their internal impedance, this element will not be introduced in the investigations of the following paragraphs.

5.2.2 Current source supply

As the previous simulations have proved the possibility to control the shape of the waveform and the magnitude of the current in the discharge by mean of the power supply, we propose to investigate in the following simulations the possibility of direct control of the current in the discharge; this is achieved with a current source supply. We consider the case of nitrogen.

Square current supply. Simulations of Figures 14 and 15 have pointed out that triangle voltage supply permits to obtain (when the discharge is in on-state) square currents; more generally, they prove that one can control the pattern of the current in the discharge by mean of a well chosen supply's voltage waveform. We propose now to consider a square current supply, applied to the whole apparatus (gas + ceramics electrodes) Figure 16b; as will be shown, the current in the discharge is flowing during quite the whole of each half-period and one can expect from this solution an interesting power transfer to the discharge and controlled current peaks at turn-on, thus avoiding filamentary regime risks.

We can remark that the current which flows in the discharge (Fig. 16d) does not exactly correspond to the supply's one (Fig. 16b); indeed, the discharge turns off when the supply's current matches a null value and voltage conditions related to V_{gas} (Fig. 16e) have to be met for the discharge to turn-on again: $\mid V_{\text{gas}} \mid > V_{\text{br}}$. During the necessary time interval to invert the gas voltage, the supply's current flows into the gas capacitor (Fig. 16c). These two sequences, appearing on each half-period of the supply, can be observed on the supply's voltage waveform (Fig. 16a). The strongest slope corresponds to the time interval where the discharge is in off state; the supply's current flows in the serial association of the capacitors: C_{ceram} and C_{gas}. The lowest slope corresponds to the on-state of the discharge: the voltage across the gas has a very small ripple (as stated in the relations Eq. (1) and Eq. (2)) and the supply's current, flowing through the C_{ceram} capacitor in serial with the gas, defines the supply's voltage: considering the energy transfer to the gas, we have to note that only the risk of transition to filamentary regime (which the model presented in this paper is unable to detect), may limit the supply's current magnitude. When this parameter is increased, the duration of the off state of the discharge decreases. Another way to match the same optimal behaviour is to minimise the value of the gas capacitor, C_{gas}, (but one should remind that the value of the breakdown voltage, V_{br}, should not be considerably increased).

Sine current supply. A practical realisation of a supply apparatus able to generate pure square currents and high voltages (Fig. 16a) is a rather hard to fulfil challenge; parasitic elements (and at first rank parasitic capacitors) drastically decay the performances. Static converters, using resonance technology, permit to deliver such high voltages and to generate quasi-sine currents. This solution is

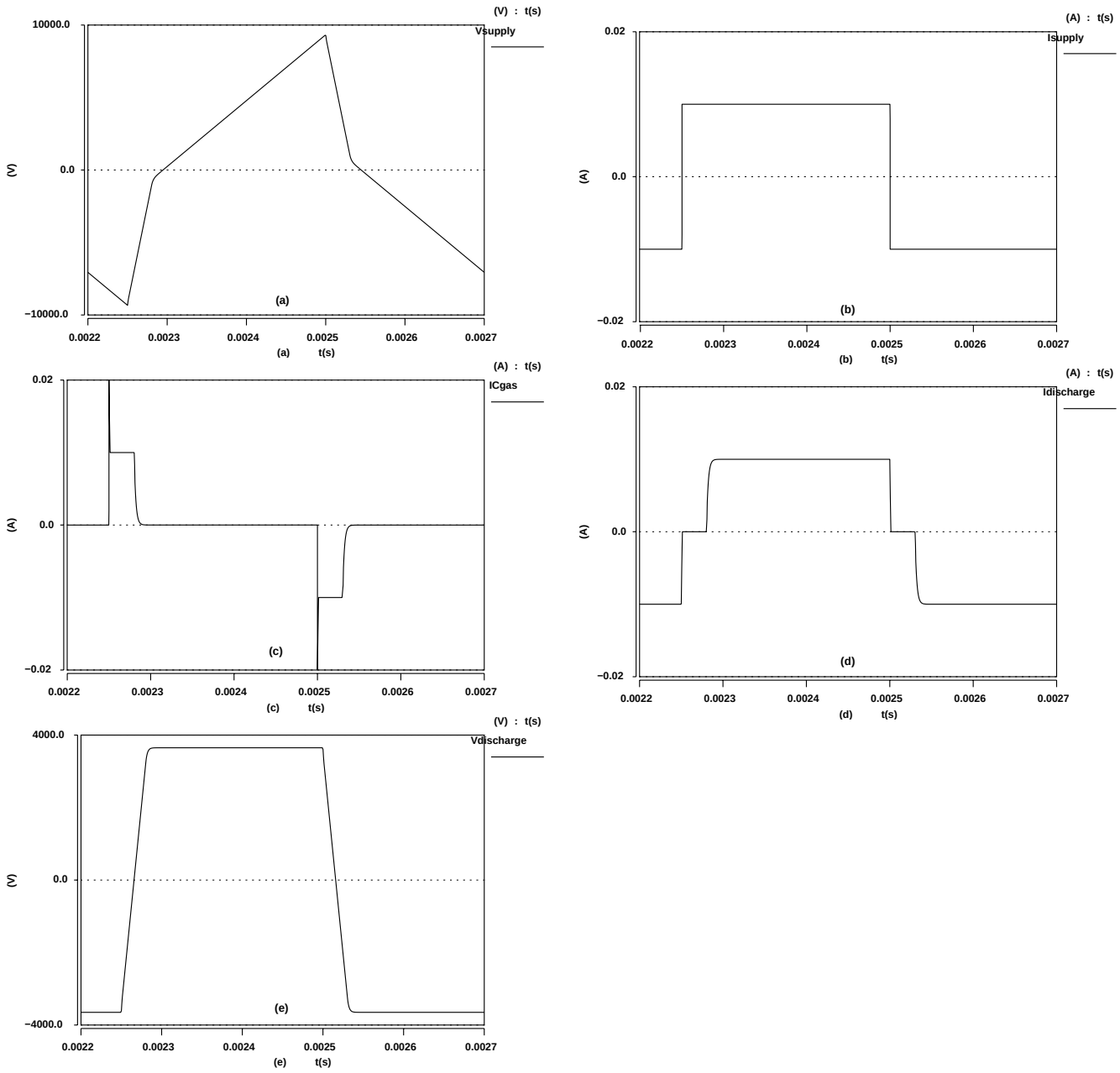

Fig. 16. Simulation in nitrogen, with square current supply ($I_{\text{peak}} = 10$ mA at 2 kHz): (a) supply's voltage, (b) supply's current, (c) current in the gas capacitor, (d) discharge's current, (e) discharge's voltage.

investigated in the following simulations: the supply consists of a sinusoidal current source (Fig. 17b).

One can observe once again the inversion sequences of the gas voltage (Fig. 17e): during these time intervals, the discharge is off and the supply's current flows in the capacitor of the gas C_{gas} (Fig. 17c).

When the discharge is on state, the current in the later is imposed by the supply (Fig. 17d).

These two sequences are also to be seen on each half period of the supply's voltage (Fig. 17a).

5.3 Validation of the model in helium

The modelling and the method for the identification of the parameters, which have been presented in the previous section, have been also validated in the case of helium. Figure 18 presents the simulation's results with supply's parameters corresponding to the operating conditions of experimental waveforms of Figure 3a. The very good accordance of the results has to be pointed out.

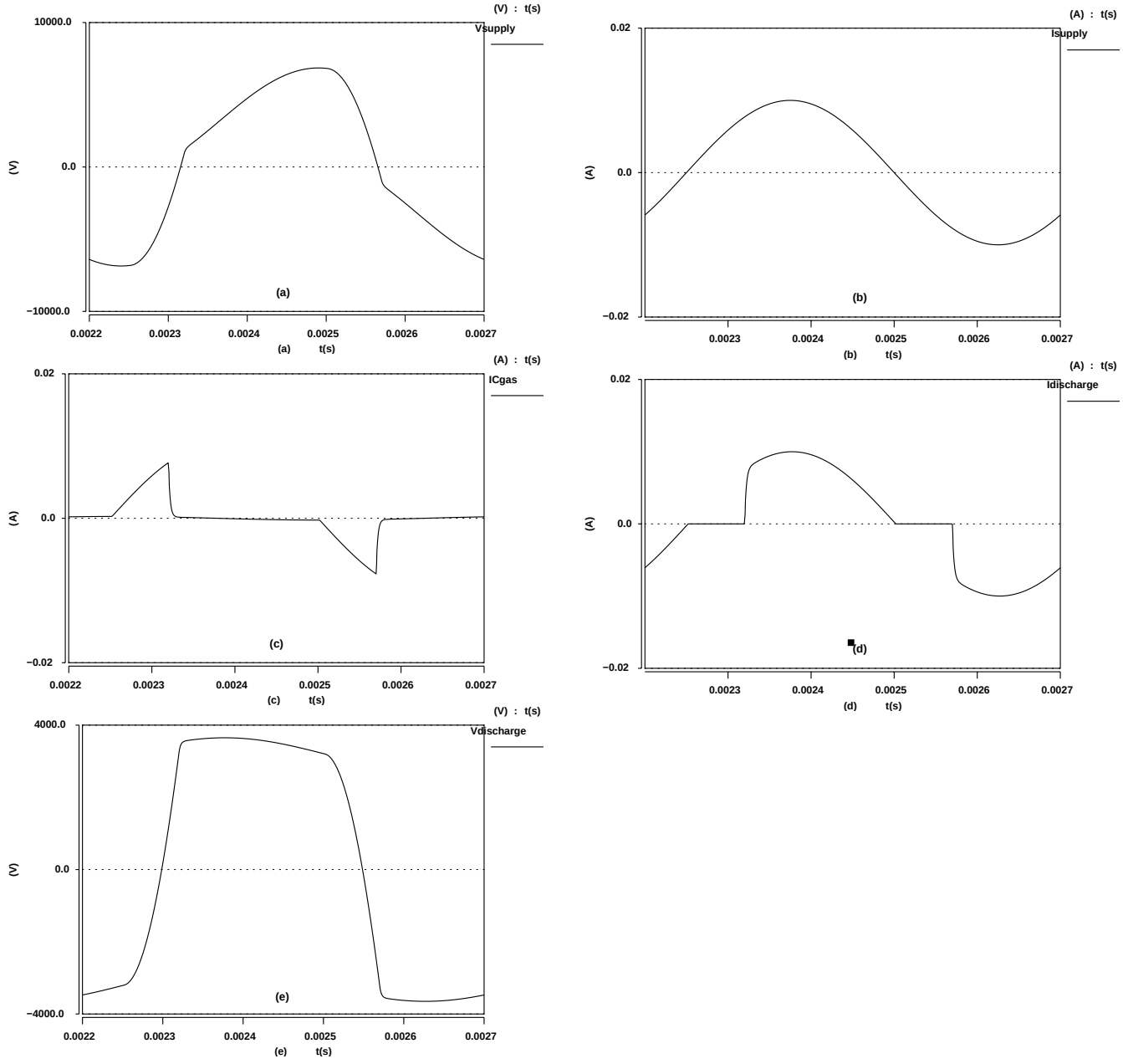

Fig. 17. Simulations in nitrogen with a sine current supply ($I_{\text{peak}} = 10$ mA at 2 kHz): (a) supply's voltage, (b) supply's current, (c) current in the gas capacitor, (d) current in the gas, (e) voltage across the gas.

6 Conclusion

This paper proposes a modelling of the homogeneous discharge, controlled by a dielectric barrier. The model is set up by mean of equivalent electrical circuits. A method for the identification of the parameters of the model on the basis of experimental waveforms is proposed; modelling and parameters identification is applied to the case of discharges in nitrogen and helium. The simulation results are showing a very good accordance with experimental results. Our approach is also exploited to exhibit the possibility of discharge's current control by mean of the electrical characteristics of the supply. On the basis of a simulation with triangle voltage supply, we point out the crucial importance of the voltage slope on the current in the discharge: it permits us to define the waveforms shape and the magnitude of the current. Then current source supply is investigated; in a first step, we consider a square current supply, which easily allows to understand and explain the obtained waveforms; in a more realistic approach, we

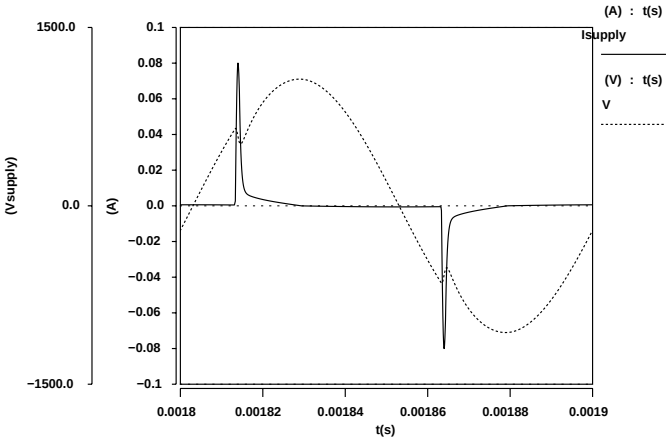

Fig. 18. Simulated waveforms: current in the discharge and supply's voltage in helium (frequency: 10 kHz).

consider in a second step a sine current supply. These two investigations point out the versatility of our model and its ability to take into account the main phenomena of the discharge mechanism as well as the influence of the supply characteristics according to the obtained performances.

The presented work has been achieved as a part of the REACTIF/ADEPLAS project, with support of the French "ministère de l'enseignement supérieur et de la recherche". Our friendly thanks to our colleagues in this project from Air Liquide, CPAT (Centre de Physique des Plasmas et de leurs Applications de Toulouse) and LGET (Laboratoire de Génie Électrique de Toulouse).

References

1. *Saber Designer User's Guide (5.1)*, Analogy Inc. Corp., 1999.
2. Masuhiro Kogoma, Satiko Okazaki, J. Phys. D **27**, 1985 (1994).
3. F. Massines, A. Rabehi, P. Decomps, R. Ben Gadri, P. Segur, C. Mayoux, J. Appl. Phys. **83**, 2950 (1998).
4. Satiko Okazaki, Masuhiro Kogoma, Makoto Uehara, Yoshihisa Kimura, J. Phys. D **26**, 889 (1993).
5. J.R. Roth, *Industrial Plasma Engineering, Volume 1 – Principles* (Institues of Physics Publishing, Bristol and Philadelphia, 1995).
6. Y. Cheron, T. Meynard, *Soft Commutation* (Chapman et al., London, 1992).